Int J Adv Manuf Technol (2016) 87:2245–2257
DOI 10.1007/s00170-016-8619-z

ORIGINAL ARTICLE

Finite element analysis for diagnosis of fatigue failure of composite materials in product development

Z. M. Bi[1] · **Donald W. Mueller Jr.**[1]

Received: 6 November 2015 / Accepted: 9 March 2016 / Published online: 23 March 2016

Abstract In contrast to homogenous materials, composite materials can be customized to achieve desirable strength-to-weight ratios, corrosion prevention, and fatigue resistances. However, the heterogeneity in composite materials brings the challenges in design, production, characterization, and testing. Trial and error practices and numerous experiments are usually required to deal with the uncertainties of composite material properties. Mathematical modeling or numerical simulations have been studied to shorten product development cycles. In this paper, we use finite element analysis (FEA) approach to diagnose the fatigue failure of composite materials. The proposed approach is novel in sense that (1) the new procedure and guideline has been developed for defining fluctuated loads in actual applications, (2) the motion simulation is conducted to characterize dynamic loads, (3) FEA is suggested as a diagnosis tool to detect design defects when failure occurs; and (4) conventional Minor's rule is expended to evaluate the fatigue life of machine elements with the consideration of both the variations of magnitudes and frequencies of stresses. A case study is provided to illustrate the analysis of the fatigue failure of products. A comparison of simulation and experimental results has verified the effectiveness of the developed approaches.

Keywords Sustainable manufacturing · Composite materials · Fatigue failures · Motion simulation · Finite element analysis

✉ Z. M. Bi
biz@ipfw.edu

[1] Department of Civil and Mechanical Engineering, Indiana University Purdue University Fort Wayne, 2101 E. Coliseum Blvd, Fort Wayne, IN 46805, USA

1 Introduction

Manufacturing systems transfer raw materials into products to meet customers and society needs. The evolutions of manufacturing systems depend on the advance of engineering materials greatly. The functionalities of both products and machine tools are constrained by the properties of applied materials; the economy of industry is no better than its best materials [8, 13, 18]. The evolution of materials was driven by economics, logistics, and the expectations of society, and the processing methods and design tools made material evolution feasible [29].

Metals and their alloys have been used as dominant engineering materials for a few of centuries. However, in recent years, their critical roles have been challenged by other materials such as plastics, ceramics, and composite materials in many applications. Note that the globalized economy is forcing enterprises to explore any opportunities in a product life cycle to expand product functionalities, improve quality, reduce cost, and shorten the delivery time [3–5, 9, 10]; using composite materials is becoming an effective strategy to achieve these goals since they can be tailored to meet various needs in specific applications [28].

Using more and more composite materials is also driven by the increasing public concern on the sustainability of our global living environment. In recent years, the concern on environmental sustainability has attracted a great deal of attention [1]. Sustainable manufacturing brings a number of new drivers for using composite materials, i.e., (1) the shortages of natural resources, (2) global warming affects, and (3) ever-increasing population and consumption of resources. It is clear that the world requires scalable solutions to deal with these challenges, and using composite materials turns into a promising solution [26]. Composite materials can be more economical, durable,

and lightweight than traditional materials. They should align well with the global trends of sustainability and energy efficiency [24, 25].

The usage of composite materials has brought significant benefits in many applications [7, 8]. For example, Tomblin [31] introduced the example of Boeing 787 for using composite materials to reduce the number of parts and increase the fuel efficiency and passenger comfortableness. The market investigation by Witten and John [34] showed that the major applications of composite materials were transportation (34 %), construction (34 %), electro/electronic (15 %), and sports/leisure (15 %) sectors. Hossain [16] evaluated the uses of composite materials in the petroleum industry, where composite materials became influential engineering materials in oilfield and surface pipeline applications. Verpoest [33] discussed the trends and challenges in developing new composite materials. The identified trends include the proliferation of carbon fibers, intelligent fiber architectures, sustainable composites, automated manufacturing, and recycling.

With the increasing use of composite materials, it is required to gain good understanding on their behaviors and design lives [14]. A composite material is defined as a macroscopic combination of two or more distinct materials having a recognizable interface between them. Smith [29] indicated that in contrast other engineering materials, composite materials can be customized to have a better strength-and-weight ratio, fatigue resistance, corrosion resistance, the possibility of having complex shapes, and reduced tooling cost and materials. However, two significant weakness of using composite materials are (1) lack of design data and tools, and (2) the uncertainties in failure predications. Critical structures and components in the applications require a special attention to evaluate the integrity of composite materials based on the design criteria of safety, quality, and reliability.

In this paper, the fatigue life of a composite material is concerned, and the numerical simulation is used to predict its fatigue life in the applications. In contrast to other existing works on modeling of composite materials, we focus on how to acquire appropriate data for the simulation. The rest of paper is organized as follows. In Sect. 2, relevant works on modeling of composite materials are discussed to identify the limitations. In Sect. 3, the systematic procedure is proposed to develop a finite element model for fatigue analysis; the importance of reliable data for valid numerical simulation is discussed. In Sect. 4, the failure diagnosis of actual product is used as the case study to illustrate the application of the proposed procedure. In Sect. 5, the simplified analytical models are developed and programmed; the results are used to verify finite element analysis (FEA) models. In Sect. 6, the presented work is summarized and the limitations are discussed.

2 Modeling of composite materials

Composite materials are inhomogeneous and anisotropic; their behaviors are very complicated which can cause multiple types of failure such as fiber fracture, cracking, fiber building, interface failure, or delamination [12]. It poses the challenges to model composite materials. Torquato [32] reviewed the modeling of physical properties of composites from the perspectives of theoretical approaches, imaging technique, and topology optimization. The discussed material properties are *elastic moduli*, *conductivity*, *thermal expansion coefficients*, *piezoelectric coefficients*, and *failure characteristics*. In this paper, the focus is put on the prediction of the fatigue life of products, which are made of composite materials. Fatigue mechanism is one of the most complicated problems when composite materials are applied. The characterization of the fatigue properties still relies on substantial tests. Limited works were available to use alternative approaches to characterize fatigue properties of composite materials [21]. For example, Mathur et al. [23] applied the artificial neural network to reduce the required experiments in the optimization of composite materials. Degrieck and Paepegem [12] discussed the major fatigue models and the methodology for predicting the fatigue life of fiber-reinforced composites; they classified fatigue models into (1) *the fatigue life model* where actual degradation mechanisms were omitted, (2) *the phenomenological models* based on residual stiffness and strength, and (3) *the progressive damage models* where the damage was quantified by measured cracks or delamination. Mao and Mahadevan [22] discussed the fatigue damage model of composite materials, the characteristics of the damage growth were especially taken into account, and it was compared with that of homogeneous materials. The proposed models were found be more accurate to fit experimental data. Liu and Mahadevan [17] developed a damage model to predict the fatigue life of laminated composite materials, and a new multiaxial index was introduced to measure the damage. One of main drawbacks of the composite materials is low repeatability of the operational characteristics. Wrobel et al. [35] illustrated the possibility of using FEA to simulate dynamic acoustic and thermal processes; their focus was on the fatigue and ageing processes of composite materials.

Numerous papers have been found on the development and the characterization of composite materials, while little attention has been paid on addressing some actual problems when composite materials are applied in products. Due to the complexity, the fatigue analysis of composite materials has not been well addressed. In this paper, the fatigue analysis has been conducted for a type of composite materials; both the analytical model and finite element model have been developed and used for designing parts made from composite materials. The detailed design of a tie rod in a spider lifter is used as a case study. Tie rods are made of fiberglass (0°/90° e-glass)

to avoid electrical shortcuts in the proposed applications. The original design of the tie rod was failure to meet the requirements of the fatigue life in this case study, and FEA is conducted to diagnose the fatigue failure.

3 Procedure of numerical simulation for fatigue analysis

FEA is one of the most effective tools in numerical simulation [2, 6, 15]. It is often the first choice when a designer encounters the difficulties in developing analytic or statistic models to find field variables in an application. As the matter of fact, finding an analytic solution is usually impossible or impractical when the actual geometries, boundary constraints, and loading conditions are considered, and FEA becomes a defact tool in the majority of engineering designs. Many software tools, such as Ansys, Comsol, Abaqus, Nastran, SolidWorks simulation, and other sophisticated packages, are commercially available for multi-disciplinary FEA applications. In this paper, we use SolidWorks to illustrate the proposed methods. Note that it is not important to select what type of simulation tool since the capacities of available tools are similar; the critical tasks for a user are to define appropriate inputs for the given problem, validate, verify, and utilize simulation results adequately.

For whatever commercial FEA code is applied, the procedure for developing and solving an FEA model is similar. As shown in Fig. 1a, the activities involved in this procedure can be classified into three phases, i.e., pre-processing, post-processing, and solving processing. While most of activities are performed by FEA software tools, users are responsible for defining an appropriate FEA problem, providing model inputs, interpreting, and verifying the results from the numerical simulations adequately. If the inputs of an FEA model are wrongly given, the obtained results from a numerical simulation could mislead designers. In contrast to relevant works focusing on modeling of composite materials, we emphasize the importance of pre-processing and post-processing. Cautious actions are planned to define boundary conditions and loads and to validate the results from simulation appropriately. In the next sections, a case study of diagnosing the fatigue failure of a product with composite materials is introduced, and the preparation of inputs and verification of the simulation results are detailed to show the application of the proposed procedure.

4 Case study—FEA for diagnosis of fatigue failure

A client company supplies parts to aerial-lift truck manufacturers. Parts are made of fiberglass (0°/90° e-glass). As shown in Fig. 2a, these parts are called as *tie rods*, and they are the part of overall truck structure to support the working platform attached on the boom. The main purpose of using composite materials for tie rods is to avoid an electrical shortcut from the workplace to the ground. The original design of tie rods was based on the static analysis; it turned out that the impact of dynamic loads was significantly underestimated. It caused a severe damage during the deployment of the prototyping lift system.

As shown in Fig. 2b, the fracture occurred to the joint between tie rod and lift base; it happened around 100 h of service. The failure diagnosis in this incident will be used as a case study in this section. FEA is used to (1) determine if the fatigue failure is the actual cause of failure in this incident, (2) choose an appropriate size the fiberglass sleeve so that no fatigue failure occurs to tie rods, and (3) ensure that one rod is strong enough to support the boom for a period of over 10 min in case that the other tie rod breaks.

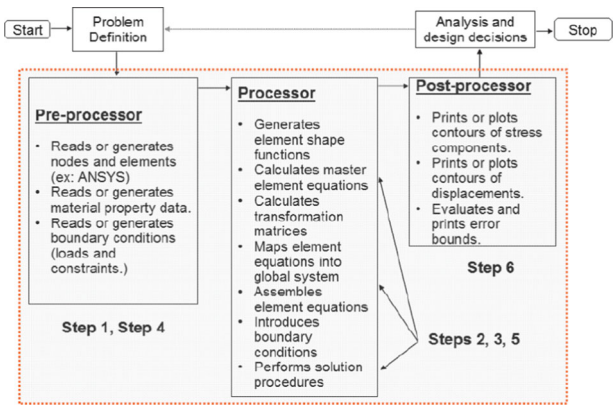

(a) FEA framework

Step 1 -Decompose : The problem domain is discretized into a collection of elements whose types of elements are defined correspondingly.
Step 2 - Develop Element Equations: Develop governing mathematic equations about field variables using direct methods, weighted residual methods or others.
Step 3 - Assembly: The equations for individual elements are assembled into a system model.
Step 4 - Apply Boundary Conditions and Loads: The interfaces of analyzed objects and environment are defined in the form of boundary conditions and loads.
Step 5 - Solve for Primary Unknowns: The system model with defined boundary conditions and loads is solved to obtain primary unknowns in elements.
Step 6 - Calculate Derived Variables: Dependent variables are calculated using obtained primary variables.

(b) Major steps and activities in FEA

Fig. 1 The procedure for developing and solving an FEA model. **a** FEA framework. **b** Major steps and activities in FEA

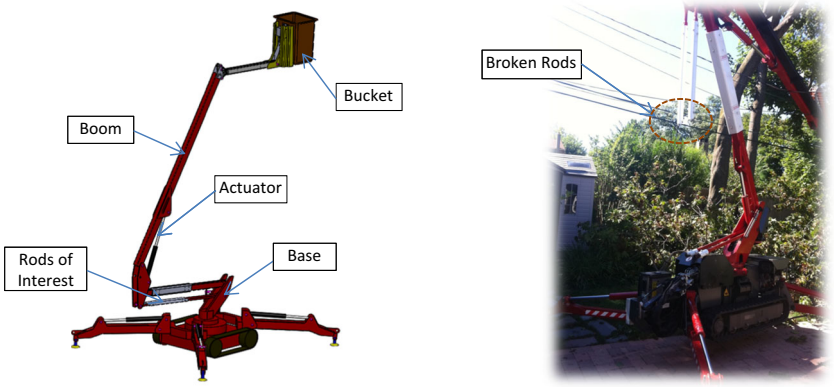

(a) Product structure (b) Part failure

Fig. 2 Product fatigue failure in case study. **a** Product structure. **b** Part failure

The procedure for developing an FEA model is shown in Fig. 1. The first step is to collect raw data of the original design problem and specify the inputs of the FEA model accordingly.

4.1 Inputs of material properties

Tie rods are made of 0°/90° e-glass, which is one of mostly used composite materials. Its material properties are publically available at a number of sources over the Internet. However, one caution should be paid to determine what material properties are used in the FEA. The properties of a composite material relate to given manufacturing processes, which can vary from one place to another. Given the fact that the client used e-glass, 50 % of fiberglass, and 0°/90° configuration, the basic properties in Table 1 were applied [27].

In the fatigue analysis, the curve of *strength–number of cycles* (S–N curve) is essential. However, the client was not capable of conducting sufficient experiments to characterize the fatigue behavior of composite materials. Available fatigue data relevant to composite materials are mostly dedicated to their applications on wind or aircraft turbines. The data from one source is often incomplete in terms of what materials and conditions in the fatigue analysis are conducted [19, 20, 30]. The closed data to meet our needs are given in Fig. 3 by Sutherland and Mandell [30] as follows.

4.2 Raw data for load definition

The other important inputs for fatigue analysis are dynamic loads. Mean and fluctuated loads on products will be determined based on the given *nominal loads*, *safety factors*, and *dynamic loads*, which are specified in the operation standards UNI EN 280:2005 “Mobile elevating work platforms - Design calculations - Stability criteria - Construction - Safety - Examinations and tests” as follows.

In conformity with the load standards of lift, the following nominal loads are considered:

- *Nominal load*: 2 persons + tools = 2 × 80 kg + 40 kg = 200 kg. In resistance, stability, and fatigue calculation, the nominal load is increased in a factor $f_1 = 1.15$, resulting in a load of 230 kg.
- *Inertia loads*: The inertial loads are assumed as $0.1 \times mp$, where *mp* is the mass of the part in movement. The direction of inertia load is the direction of movement.
- *Manual forces*: A force of 20 kg × 1.1 = 22 kg (for each person in cage) is considered acting on cage hand rail. These forces are considered acting in the worst possible direction. The manual forces are not considered combined with inertia forces.
- *Wind forces*: The wind forces, in operating condition, are considered acting with horizontal direction for a reference pressure of 100 N/m^2 × 1.1 = 110 N/m^2.

In conformity with the safety standards, UNI CEN/TS 13001-3-1:2005 “Cranes - General design - Part 3–1: Limit states and proof of competence of steel structures,” the following safety factors are considered (Table 2).

According to the standard UNI EN 280:2005, the spider lift is considered to have a platform’s life of 10 years, which

Table 1 Basic material properties of tie rod [27]

	Young’s modulus	Poisson ratio	Tensile strength	Yield strength	Compression strength	Density
50 % fabric, dry, room temperature, e-glass	24GPa	0.2	440 MPa	400 MPa	425 MPa	1.900 kg/m^3

Sample No.	N	$S_f(R=-1)$
1	1	400MPa
2	100	325MPa
3	1000	275MPa
4	10000	210MPa
5	100000	149MPa
6	1000000	110MPa

(a) S-N Dataset

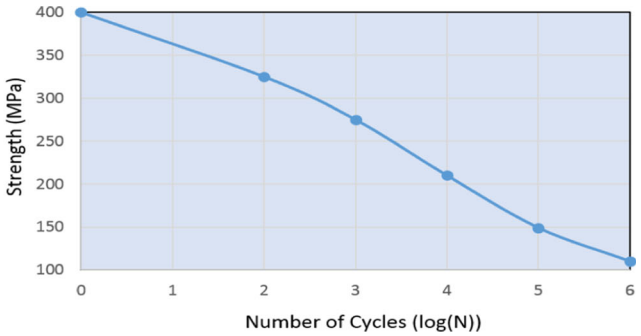

(b) S-N Curve

Fig. 3 The S–N curve in FEA [30]. **a** S–N dataset. **b** S–N curve

corresponds to 100,000 cycles of dynamic loads. All parts of platform are considered to have the following load spectrum:

- 16,667 cycles with max load in cage and maximum outreach $P_i = P_{max}$
- 16,667 cycles with max load in cage and 1/2 maximum outreach $P_i = (0.5)\ P_{max}$
- 16,667 cycles with load in cage = 0.8 × maximum load and maximum outreach $P_i = (0.8)\ P_{max}$
- 16,667 cycles with load in cage = 0.8 × maximum load and 1/2 maximum outreach $P_i = (0.4)\ P_{max}$
- 16,667 cycles with load in cage = 0.7 × maximum load and maximum outreach $P_i = (0.7)\ P_{max}$
- 16,667 cycles with load in cage = 0.7 × maximum load and 1/2 maximum outreach $P_i = (0.35)\ P_{max}$

Based on the fatigue verification standards UNI EN 1993-1-9, the probability of survival of 95 % is applied; it is found to be $K_R = 0.868$ [11].

4.3 Force analysis to define dynamic loads

To determine the stress distribution in a tie rod, the force applied on the spider lift must be analyzed to characterize fluctuated loads. For the sake of safety, the extreme conditions leading to the maximized stress of rod are specially considered. The stresses are calculated based on the maximized loads on rods. The safety factors under a static maximized load are determined for three possible failure modes.

Table 2 The required safety factors for spider lift

Components	Safety factor (n_f)
Long beams (buckling/bulging)	1.7
Structures	1.48
Bolts	1.48
External loads	1.15

The assembly of the upper boom is isolated from the spider lift, and its free-body diagram (FBD) is shown in Fig. 3. The whole body has (1) the reaction forces from rods and low booms at A and O, respectively, (2) the self-weight of upper boom at gravity center B, (3) the load of bucket at C, and the net wind force applied at (x_c, y_c). These forces must be balanced in operation.

Taking position O as the reference center, the condition of the moment balance with respect to O leads to

$$F_R \cdot |OA| \cdot \sin\theta_1 - W_S \cdot x_B - W_B \cdot x_C \pm (p_w \cdot A_B) \cdot y_C = 0 \tag{1}$$

Equation (1) describes the dependence of tensional force F_R in two rods with other variables. The physical meanings of these variables, values or ranges, are given in Table 3 and Figs. 3 and 4. Note that the suggested values and ranges are recommended by users for their applications.

Once the variables in Table 4 are given, F_R can be found as

$$F_R = \frac{W_S \cdot x_B + W_B \cdot x_C \mp (p_w A_B) \cdot y_C}{|OA| \cdot sin\theta_1} \tag{2}$$

The extreme loading conditions of the tie rods are illustrated in Fig. 5a, b. Accordingly, the maximal and minimal tensional forces in two rods can be determined as,

$$F_{R,\max} = \frac{W_S \cdot x_{B,\max} + W_B \cdot x_{C,\max} + (p_w A_B) \cdot y_{C,\min}}{|OA| \cdot sin\theta_{1,min}} \tag{3}$$

$$F_{R,\min} = \frac{W_S \cdot x_{B,\min} + W_B \cdot x_{C,\min} + (p_w A_B) \cdot y_{C,\max}}{|OA| \cdot \sin\theta_{1,\max}} \tag{4}$$

Based on six scenarios specified by the user, the characteristics of dynamic loads are determined as follows.

- Scenario 1: 16,667 cycles with max load in cage and maximum outreach $W_B = W_{B,max}$

$$F_{R,(S1,\min)} = \frac{W_S \cdot x_{B,\min} + W_{B,\max} \cdot x_{C,\min} - (p_w A_B) \cdot y_{C,\min}}{|OA| \cdot sin\theta_{1,max}} \tag{5}$$

Table 3 Design variables and suggested ranges

	Description	Suggested values or ranges
F_R	The tensional force in two tie rods	Determined by Eq. (2)
W_S	Self-weight of the upper beam and bucket	673.5 kg (the assembly model)
W_B	Max load in bucket	1.5 * 272.16 kg
P_W	Wind pressure	100 N/m^2
A_B	Area which carries wind	1.1 m^2
θ_1	Angle between *OA* and tensional force	40.72°–90°
x_B	Distance from O to B along X	1.13 m—3.58 m
x_C	Distance from O to C along X	3.38 m—6.49 m
y_C	Distance from O to C along Y	0.00 m—6.58 m
OA	The distance from *O* to *A*	0.3 m
Do	The outside diameter of rod	0.06985 m
Di	The inside diameter of rod	0.0508 m
Dh	The size of bolt hole	0.01349 m
t	Thickness of rod wall	0.009525 m
d	The shortest distance from hole to rod end	0.04762 m

$$F_{R,(S1,\max)} = \frac{W_S{\cdot}x_{B,\max} + W_{B,\max}{\cdot}x_{C,\max} + (p_w A_B){\cdot}y_{C,\max}}{|OA|{\cdot}\sin\theta_{1,\min}} \quad (6)$$

- Scenario 2: 16,667 cycles with max load in cage and 1/2 maximum outreach $W_B = (0.5) \times W_{B,max}$

$$F_{R,(S2,\min)} = \frac{W_S{\cdot}x_{B,\min} + (0.5W_B){\cdot}x_{C,\min} - (p_w A_B){\cdot}y_{C,\min}}{|OA|{\cdot}\sin\theta_{1,\max}} \quad (7)$$

$$F_{R,(S2,max)} = \frac{W_S{\cdot}x_{B,max} + (0.5W_B){\cdot}x_{C,max} + (p_w A_B){\cdot}y_{C,max}}{|OA|{\cdot}sin\theta_{1,min}} \quad (8)$$

- Scenario 3: 16,667 cycles with load in cage = 0.8 × maximum load and maximum outreach $W_B = (0.8) \times W_{B,max}$

$$F_{R,(S3,min)} = \frac{W_S{\cdot}x_{B,min} + (0.8W_B){\cdot}x_{C,min} - (p_w A_B){\cdot}y_{C,min}}{|OA|{\cdot}sin\theta_{1,max}} \quad (9)$$

$$F_{R,(S3,\max)} = \frac{W_S{\cdot}x_{B,\max} + (0.8W_B){\cdot}x_{C,\max} + (p_w A_B){\cdot}Y_{C,\max}}{|OA|{\cdot}sin\theta_{1,min}} \quad (10)$$

- Scenario 4: 16,667 cycles with load in cage = 0.8 × maximum load and 1/2 maximum outreach $W_B = (0.4) \times W_{B,max}$

$$F_{R,(S4,\min)} = \frac{W_S{\cdot}x_{B,\min} + (0.4W_B){\cdot}x_{C,\min} - (p_w A_B){\cdot}y_{C,\min}}{|OA|{\cdot}sin\theta_{1,\max}} \quad (11)$$

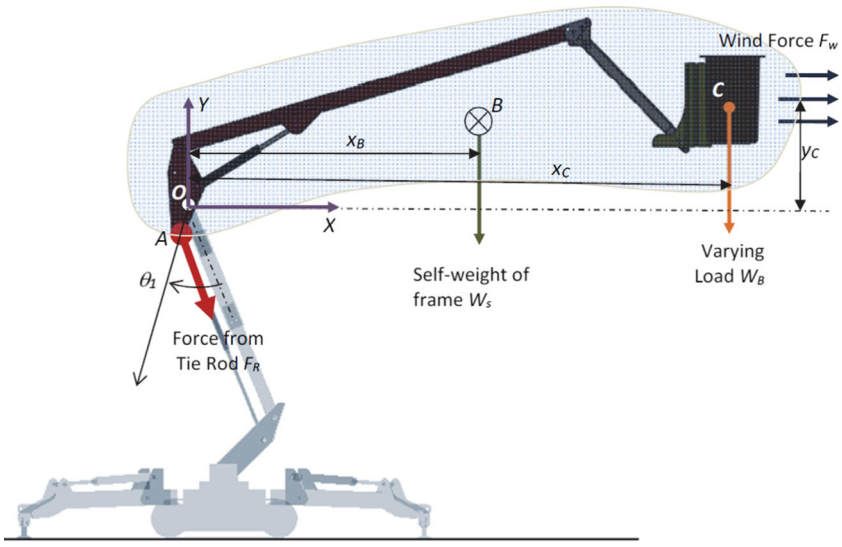

Fig. 4 Forces applied on the assembled upper boom

Table 4 Failure modes, stresses, and safety factors

Failure mode	Stress equation	Safety factor
Tensile failure	$\sigma_{average} = \frac{F_R/2}{\pi\left[(D_0/2)^2-(D_i/2)^2\right]-Dh*(D_0-D_i)_Y}$	$n_{f,t} = \frac{S_Y}{K_t \cdot \sigma_{average}}$
Bearing failure	$\sigma_{compression} = \frac{(F_R/(\text{number of rods}))/(\text{number of walls of a hole})}{(\text{Diameter of Bolt})*(\text{thickness of wall})*2}$	$n_{f,c} = \frac{S_C}{K_t \cdot \sigma_{compression}}$
Tear-out failure		
Shear failure	$\tau_{shear} = \frac{(F_R/(\text{number of rods}))/(\text{number of walls of a hole})}{2*(\text{thickness of wall})*(\text{the shortest distance from a hole to the end of rod})}$	$n_{f,s} = \frac{S_Y/2}{K_t \cdot \tau_{shear}}$

$$F_{R,(S4,\max)} = \frac{W_S \cdot x_{B,\max} + (0.4W_B) \cdot x_{C,\max} + (p_w A_B) \cdot y_{C,\max}}{|OA| \cdot \sin\theta_{1,\min}} \quad (12)$$

- Scenario 5: 16,667 cycles with load in cage = 0.7 × maximum load and maximum outreach $W_B = (0.7) \times W_{B,max}$

$$F_{R,(S5,\min)} = \frac{W_S \cdot x_{B,\min} + (0.7W_B) \cdot x_{C,\min} - (p_w A_B) \cdot y_{C,\max}}{|OA| \cdot \sin\theta_{1,\max}} \quad (13)$$

$$F_{R,(S5,\max)} = \frac{W_S \cdot x_{B,\max} + (0.7W_B) \cdot x_{C,\max} + (p_w A_B) \cdot y_{C,\max}}{|OA| \cdot \sin\theta_{1,\min}} \quad (14)$$

- Scenario 6: 16,667 cycles with load in cage = 0.7 × maximum load and 1/2 maximum outreach $W_B = (0.35) \times W_{B,max}$

$$F_{R,(S6,\min)} = \frac{W_S \cdot x_{B,\min} + (0.35W_B) \cdot x_{C,\min} - (p_w A_B) \cdot y_{C,\min}}{|OA| \cdot \sin\theta_{1,\max}} \quad (15)$$

$$F_{R,(S6,\max)} = \frac{W_S \cdot x_{B,\max} + (0.35W_B) \cdot x_{C,\max} + (p_w A_B) \cdot y_{C,\max}}{|OA| \cdot \sin\theta_{1,\min}} \quad (16)$$

Based on the data in Table 4 and Eqs. (5–16), the load history on two tie rods can be determined as shown in Fig. 6.

4.4 FEA solutions to original design

FEA has been conducted in the Simulation module of the Solid Works. Since inside rod does not carry any tensional load, it has been excluded in the analysis. Besides, due to the symmetric nature of tie rods, a half of the tie rod is taken into consideration to reduce the computation. The obtained results from static analysis and fatigue analysis are shown in Figs. 7 and 8, respectively.

In the static analysis, the inputs of material properties are given by Table 1. In defining the static load, the

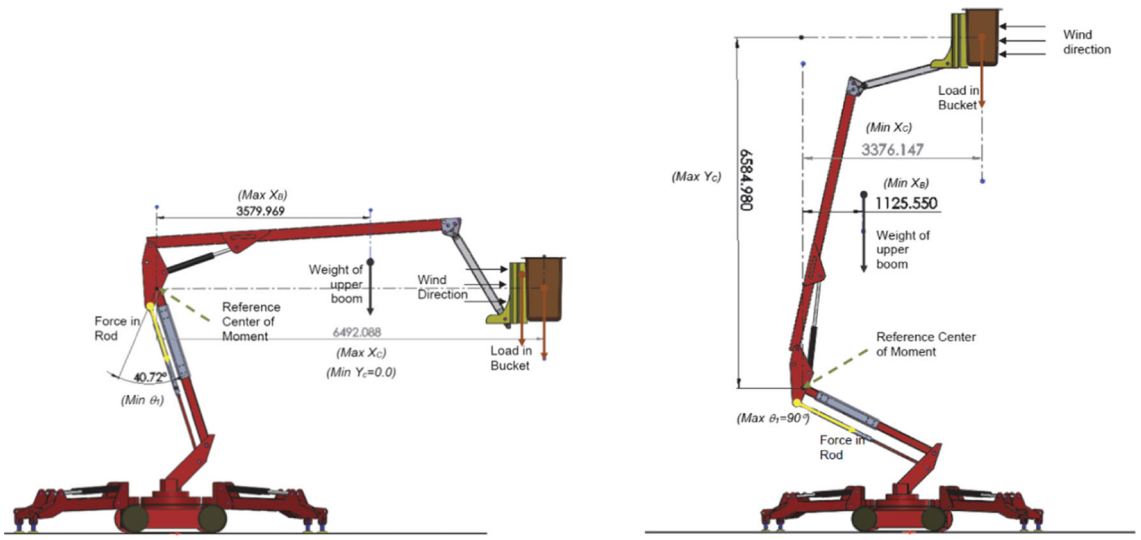

(a) Position of tie rod with a maximal load (b) Position of tie rod with a minimal load

Fig. 5 Positions of tie rods at extreme loading conditions. **a** Position of tie rod with a maximal load. **b** Position of tie rod with a minimal load

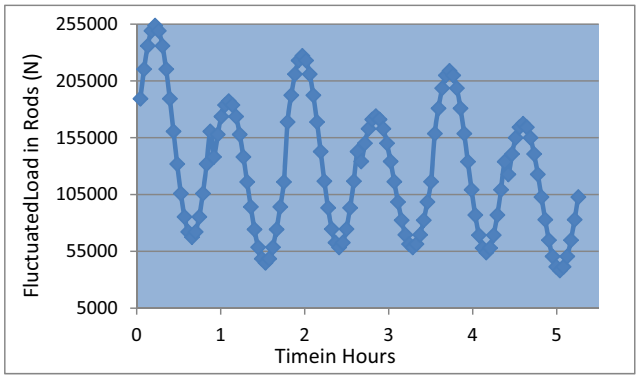

Fig. 6 History of dynamic load

external loads are applied on the hole walls of six fasteners evenly; therefore, the force on each wall is the 1/12 of the total force applied on two tie rods. The direction of the force is along the axis of the tie rod. In defining the boundary conditions, one roller/slider boundary condition is applied to the symmetric face in the middle of a tie rod to reduce computation. In the meshing process, 3D tetrahedral elements are used for meshing, and the resulted mesh is illustrated in Fig. 7a. It included a total of 326,280 nodes and 208,730 elements. The FEA solution tells that the maximum stress in Fig. 7b happens at the middle edges of the last bolt; the corresponding safety factor at the critical position in Fig. 7c is 2.02.

In fatigue analysis, the S–N curve in Fig. 3 was input as the fatigue properties of the tie rods. In defining the dynamic loads, the six scenarios illustrated in Sect. 4.3 have been processed and integrated as the inputs of the load history, and the loads are normalized accordingly in Fig. 8a. In addition, the default stress intensity is used to evaluate the reverse stress of fatigue analysis. The Goodman criterion is used to take into account the mean stress. The fatigue strength reduce factor is given as

$$K_f = K_R{*}K_c{*}K_d = 0.59024 \tag{17}$$

where

$K_R = 0.868$ is the factor of reliability of 95 %
$K_c = 0.85$ is axial load factor
$K_d = 0.80$ is the distribution factor considering the variant of distribution over three bolts.

The distribution of the life cycles over the tie rod is shown in Fig. 8b. The position corresponding to the maximized static stress has the shortest life cycle of 14.82 blocks. Accordingly, the running hour without the failure is 77.90 h.

4.5 FEA solutions to new design

The developed FEA model has been simulated for new dimension obtained based on the analytical model. As suggested by the analytic analysis in Sect. 5, the diameter of a tie rod should be larger than 0.07905 m to meet the expectation of the fatigue life. FEA is conducted to predict the fatigue life of this revised dimension. The only change in the FEA is the diameter of the tie rod; the distributions of the von Mises stress, safety factor, and fatigue life block from static analysis and fatigue analysis are shown in Fig. 9a–c, respectively. Accordingly, the expected number of years of the tie rod with new dimension is 15.35 (years). It indicates that the tie rod with new dimension meets the expectation of over 10-year fatigue life.

To ensure one rod is capable of supporting the boom for a period of over 10 min if the other tie rod breaks. The original FEA is revised by applying the doubled loads on the part. The results of static and fatigue analysis are shown in Fig. 10. The distributions of the von Mises stress, safety factor, and fatigue life block for the new model are shown in Fig. 10a– c, respectively. Accordingly, the expected fatigue life with one tie rod is 20.92 (minutes). It indicates that one tie rod can sustain

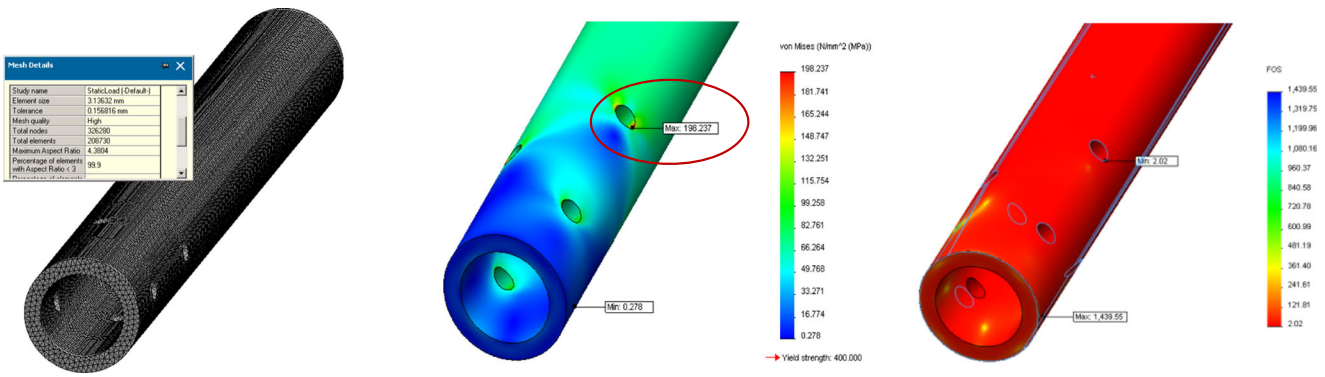

(a) Meshed part (b) von Mises stress (c) Safety factor

Fig. 7 Result of FEA static analysis. **a** Meshed part. **b** von Mises stress. **c** Safety factor

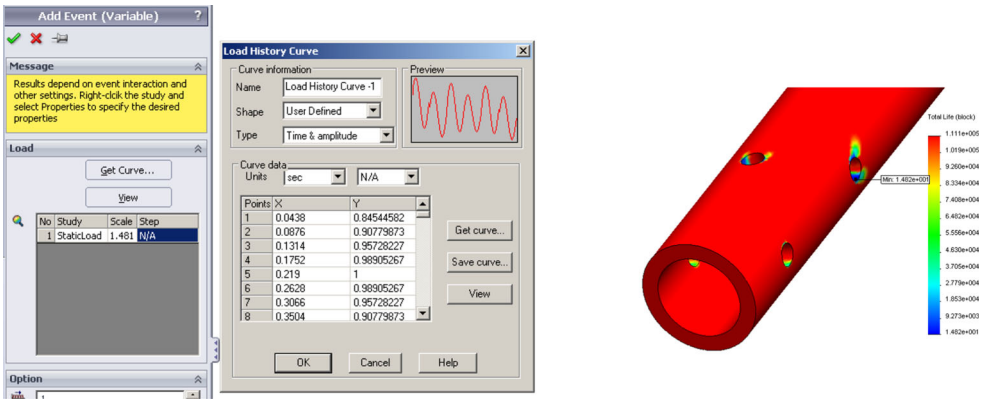

(a) Input of dynamic loads (b) Fatigue life

the boom for more than 10 min after a break happens to the other rod.

5 Verification via analytic modeling and experiment

One critical step in the post-processing of FEA is the verification. It is especially important when FEA is applied to support the design of actual products. The verification can be performed based on simplified analytical models or experimental data. Since the parts in this case study can be simplified as a binary element, a simplified model can be used to estimate the fatigue life of the part using analytical approaches. In addition, the case study was how the failure diagnosis of an actual part; some recorded data can be utilized to verify the FEA results from Sect. 4.

5.1 Analytic models and results

For static analysis, each rod in Fig. 1 can be treated as a two-force element in Fig. 11; only axial tensional load is involved. Once the pulling force F_R is found, the corresponding stress within the tie rod can be calculated and can be estimated; it is mainly determined by the area of the cross section shown in Fig. 12. The minimal cross section includes two holes of bolts.

The stress concentration has to be taken into consideration at the positions of bolts. Therefore, an individual FEA has been conducted to obtain the stress concentration factor under an axial loading condition. The stress concentration factor is found as 2.35. The tie rods are connected to the base by bolts, and Fig. 13 gives four possible failure modes. The corresponding safety factors against these failures are evaluated in Table 4. The equations are programed in the Matlab. With the maximized load on the tie rod of 253,665 N, the obtained safety factors against four failure modes are given in Table 5.

The application has varying amplitude loads. To predict the fatigue life analytically, the Minor's rule is used to take into account of the variable fluctuated load:

$$\frac{n_1}{N_1}+\frac{n_2}{N_2}+\frac{n_3}{N_3}+\cdots\leq\frac{1}{Df_{fatigue}} \tag{18}$$

n_i is the number of cycles at stress level σ_i
N_i is the number of cycles to failure at stress level σ_i
$Df_{fatigue}$ is the safety factor under varying amplitude loads

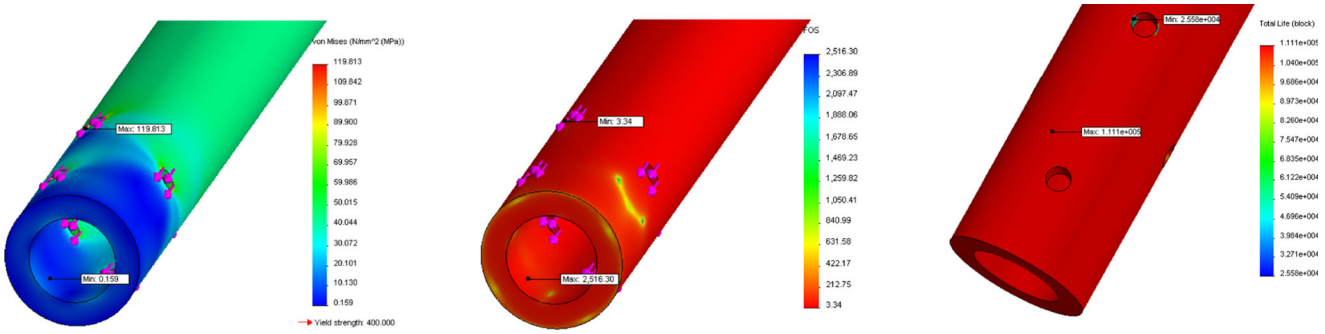

(a) von Mises stress (b) Safety factor (c) Fatigue life

Fig. 9 Static and fatigue analysis of part with new diameter. **a** von Mises stress. **b** Safety factor. **c** Fatigue life

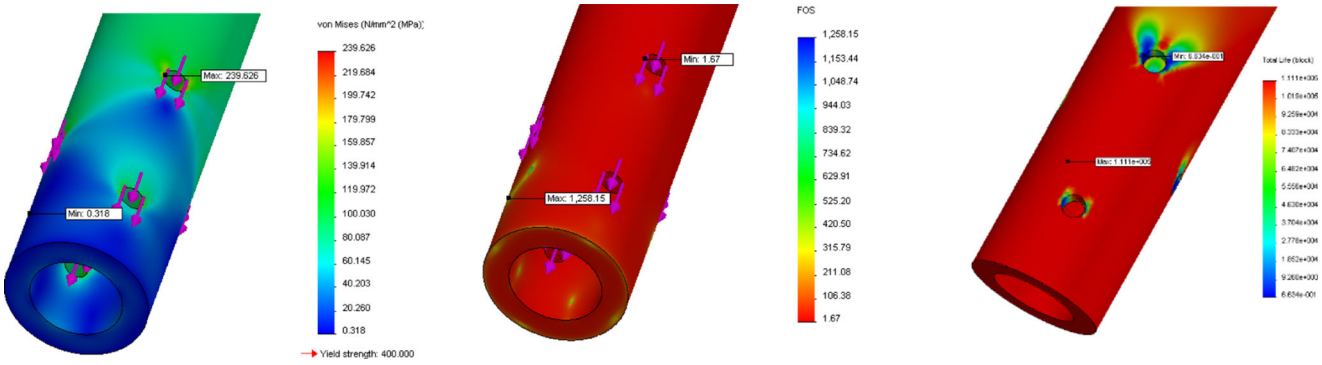

Fig. 10 Static and fatigue analysis when one rod is broken. **a** von Mises stress. **b** Safety factor. **c** Fatigue life

Since six scenarios are not under the fully reversed stress conditions, the Goodman's equation is applied to find the equivalent reverse stress $S'_{f,i}$ at a stress level ($\sigma_{m,\,i}$, $\sigma_{a,\,i}$):

$$\frac{\sigma_{a,i}}{\sigma_{f,i}} + \frac{\sigma_{m,i}}{S_{ut}} = 1 \tag{19}$$

where

$\sigma_{m,i}$ and $\sigma_{a,i}$	are the mean and alternating stress at scenario i
S_{ut}	is the ultimate strength
$\sigma_{f,i}$	is the equivalent reverse stress.

Equation (19) gives the equivalent reverse stress as

$$\sigma_{f,i} = \frac{\sigma_{a,i}}{1-\sigma_{m,i}/S_{ut}} \tag{20}$$

Thus, the number of cycles at the stress level ($\sigma_{m,\,i}$, $\sigma_{a,\,i}$) is

$$N_i = \left(\frac{\sigma_{f,i}}{a}\right)^{1/b} \tag{21}$$

The coefficients in Eq. (21) are defined based the data in Fig. 3 as,

$$a = \frac{\left(\left(S_f^i\right)_{10^3}\right)^2}{\left(S_f^i\right)_{10^6}} = 687.5MPa \tag{22}$$

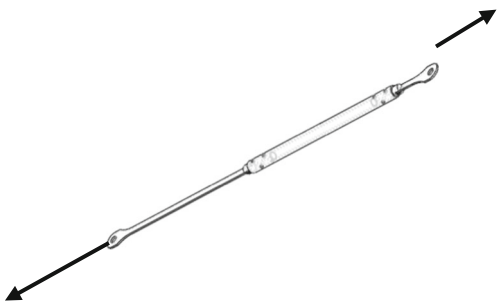

Fig. 11 Tie rod as a two-force member

where $\left(S_f^i\right)_{10^3} = 275MPa$, $\left(S_f^i\right)_{10^6} = 110Mpa$ according to Fig. 3; therefore,

$$b = -\frac{1}{3}\log\frac{\left(S_f^i\right)_{10^3}}{\left(S_f^i\right)_{10^6}} = -0.13265 \tag{23}$$

Based on Eqs. (5–16), the mean and reverse loads can be defined, and Eqs. (18–23) can be further used to evaluate corresponding stresses and the fatigue life in six scenarios. The results are summarized in Table 6. Recalling the predicted life of 77.90 h from FEA in Sect. 4.4, the discrepancy of simulation and analytic results is less than 10 %.

To suggest the new dimension of the tie rod for the expected fatigue life of 10 years with two rods and 10 min with one rod when the other rod is broken, an optimization model is developed based on Eqs. (5–23) where the rod diameter is treated as the design variable. The optimized diameter of the rod is Do = 0.07905 m. The results of new tie rod in six scenarios are summarized in Table 7. In the similar way, assuming that the loads are doubled and applied on a single rod, the

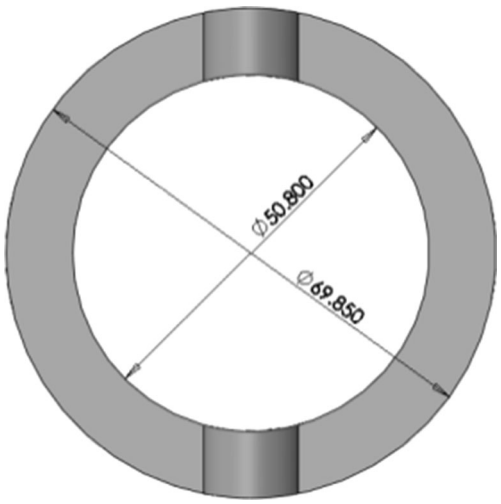

Fig. 12 Cross section of rod with minimized area

Fig. 13 Failure modes of bolted fasteners [11]. **T** tensile failure. **b** Bearing failure. **c** Tensile tear-out. **d** Shear tear-out

predicted time of one rod to support the entire boom is 11.00 min, which is relatively lower in comparison with 20.92 min from FEA simulation. Since the calculation of life cycles involves the exponential operations, which is very sensitive to digital roundups, the comparison of two results still shows the great consistence.

5.2 Summary of verifications

Both the analytic models and numerical FEA model have been developed to conduct static and fatigue analysis of tie rods. The comparison of the results is summarized as follows:

1. The existing design of tie rod failed to meet the expected fatigue life. The expected life from the analytical model is 70.77 h, and that from FEA model is 77.90 h. These results are consistent with the actual life of the broken part with a failure happening at 100 h. However, more uncertainties (modification factors) should be taken into consideration if the corresponding data become available. Possible discrepancy could be caused by (a) the self-weight of the assembled upper boom, which has a great impact on the load of tie rods, and (b) the material properties of the actual part.
2. The origin design of tie rods included obvious defects, which led to the fracture incident in the deployment of the prototyping lifter. The static analysis of the analytical model has confirmed that the safety factor for the failure of bearing factor 1.07 is below the expected safety factor 1.48 in the original design.
3. An optimization based on the analytical model has shown that the dimension of tie rod must be over ϕ79.05 mm without the consideration of uncertainties. This size is bounded by the condition that one rod under a full load should sustain the lift over 10 min. The corresponding fatigue safety factor from the analytical model is 1.3, which corresponds to 13.68 years of the operational life. The sustaining time with one rod is 10.996 min.
4. The finite element analysis for the rod part with the new dimension has confirmed that the outside dimension of the tie rod with ϕ79.05 mm might meet the requirements: The expected fatigue life is 15.35 years and the sustaining time with one rod under a full load is 20.92 min. The results from the FEA reasonably agree with these from the developed analytical model.

Table 5 Safety factors against four failure modes under maximized static load

Failure mode	Max stress (MPa)	Strength	Safety factor
Tensile failure	192.64	S_Y	2.08
Bearing failure	386.84	S_C	1.10
Tear-out failure			
Shear failure	54.78	$S_Y/2$	3.65

6 Conclusion

In this paper, we discussed the requirements of sustainable manufacturing to emphasize the importance of using composite materials in modern manufacturing. We conducted the literature review on modeling of composite materials to identify challenges in this field. For numerical simulation of composite materials, we found that relevant works emphasized the modeling of composite materials, while the work on how to develop valid numerical models for specific applications is lacking. To address this concern, we proposed a systematic procedure of FEA modeling, and we put our focus on pre-processing and post-processing. In particular, we discussed

Table 6 Dynamic loads, stresses, and predicted lives for original design

Scenario	Mean force (N)	Reverse force (N)	Mean stress (MPa)	Reverse stress (MPa)	Equivalent reverse stress (MPa)	Predicted life
1	160,630	93,035	121.98	70.65	477.26	13.46
2	116,148	71,114	88.20	54.00	240.22	(blocks)
3	142,837	84,267	108.47	63.99	358.01	0.0081
4	116,276	57,705	88.30	43.82	195.12	(years)
5	133,941	79,882	101.72	60.66	312.53	70.77
6	102,803	64,537	78.07	49.01	197.75	(hours)

Table 7 Dynamic loads, stresses, and predicted lives for new design

Scenario	Mean stress (MPa)	Reverse stress (MPa)	Equivalent reverse stress (MPa)	Predicted life
1	75.54	43.75	172.53	22,806.4 (blocks) 13.68 (years) 119,870 (hours)
2	54.62	33.44	111.06	
3	67.17	39.63	145.37	
4	54.68	27.14	90.16	
5	62.99	37.57	133.16	
6	48.35	30.35	96.23	

how to define dynamic loads and verify the fatigue analysis results. The procedure was implemented to diagnose the fatigue failure of an actual part and generate new design solution to meet the expected fatigue life. The comparison of the results from simulation and analytical models has shown the effectiveness and reliability of the proposed procedure.

While the procedure of FEA modeling was especially developed for fatigue analysis of composite materials, readers should find the presented guidance in modeling helpful to conduct FEA for the products with conventional materials in many other applications. The importance of acquiring appropriate dynamic loads and verifying the fatigue life adequately can never be over-emphasized. We believe that small- and medium-size enterprises (SMEs) could benefit from the presented work to provide better services for customized products. The design expertise at SMEs is generally lacking, and it is profit prohibiting in performing rigorous design activities to eliminate all design defects. It is more practical to make products and achieve the customer satisfaction by service. The presented work directs a practical way to implement such a strategy cost-effectively.

References

1. Bi ZM (2011) Revisit system architecture for sustainable manufacturing. J Sustain 3(9):1323–1340
2. Bi ZM (2011) Design and simulation of dust extraction for composite drilling. Int J Adv Manuf Technol 54(5–8):629–638
3. Bi ZM, Kang B (2014) Sensing and responding to the changes of geometric surfaces in flexible manufacturing and assembly. Enterp Inform Syst 8(2):225–245
4. Bi ZM, Wang L (2012) Energy modeling of machine tool for optimization of machine setup. IEEE Trans Autom Sci Eng 9(3):607–613
5. Bi, Z. M., and Wang, L., (2013). Chapter 5: Manufacturing Paradigm Shift towards Better Sustainability, in Cloud Manufacturing, Springer-Verlag London, ISBN: 978-1-4471-4934-7, doi: 10.1007/978-1-4471-4935-4_5
6. Bi ZM, Gruver WA, Zhang WJ, Lang SYT (2006) Automated modeling of modular robotic configurations. Robot Auton Syst 54:1015–1025
7. Bi ZM, Lang SYT, Shen WM (2008) Reconfigurable manufacturing systems: the state of the art. Int J Prod Res 46(4):967–992
8. Bi, Z. M., Hinds, B., Jin, Y., Gibson, R., and McToal, P. (2009). Drilling Processes of Composites-The State of the Art," in Drilling of Composite Materials, Nova Science Publisher, ISBN: 978-1-60741-163-5, pp.137-171.
9. Bi ZM, Xu LD, Wang C (2014) Internet of things for enterprise systems of modern manufacturing. IEEE Trans Ind Inform 10(2):1537–1546
10. Bi ZM, Pomalaza-Raez C, Singh Z, Nicolette-Baker A, Pettit B, Heckley C (2014) Reconfiguring machines to achieve system adaptability and sustainability: a practical case study. Proc Inst Mech Eng Part B-J Eng Manuf 228:1676–1688
11. Budynas, R., Nisbett, J. K. (2013) Shigley's Mechanical Engineering Design, 9th Edition, ISBN: 978-0-07-352928-8, McGraw Hill
12. Degrieck J, van Paepegem W (2001) Fatigue damage modeling of fibre-reinforced composite materials: review. Appl Mech Rev 54(4):279–300
13. Ferguson, C., (2014) Historical Introduction to the Development of Material Science and Engineering as a Teaching Discipline. http://www.materials.ac.uk/pub/materials-history-intro.pdf
14. Firehole Composites (2010) Fatigue Life Prediction in Composite Materials, http://www.firehole.com/documents/WP_Fatigue-Life-Prediction-in-Composite-Materials.pdf
15. Gupta KK, Meek JL (1996) A brief history of the beginning of the finite element method. Int J Numer Methods Eng 39:3761–3774
16. Hossain ME (2011) The current and future trends of composite materials: an experimental study. J Compos Mater 45(20):2133–2144
17. Liu Y, Mahadevan S (2005) Probabilistic fatigue life prediction of multidirectional composite laminates. Compos Struct 69:11–19
18. Loftas AAG (1966) Advances in materials science. University of London Press, London
19. Mandell, J. F., Samborsky, D. D., Combs, D. W., Scott, M. E., Cairns, D. S. (1998) Fatigue of Composite Material Beam Elements Representative of Wind Turbine Blade Substructure, National Renewable Energy Laboratory, Report for Contract No. DE-AC36-83CH10093 1998, www.abdmatrix.com/phcdl/upload/fatigue/Fatigue%20of%20Composite%20Material%20Beam%20Elements%20Representative%20of%20Wind%20Turbine%20Blade%20Substructures.pdf
20. Mandell, J. F., Samborsky, D. D., Agastra, P. (2008). "Composite Materials Fatigue Issues in Wind Turbine Blade Construction", www.coe.montana.edu/composites/documents/SAMPE%202008.pdf
21. Mandell, J. F., Samborsky, D. D., Wahl, N. K., Sutherland, H. J. (2014) Testing and Analysis of Low Cost Composite Materials under Spectrum Loading and High Cycle Fatigue Conditions, http://windpower.sandia.gov/other/ICCM14_Mandell_Testing.pdf
22. Mao H, Mahadevan S (2002) Fatigue damage modelling of composite materials. Compos Struct 58(4):405–410
23. Mathur, S., Gope, P. C., Sharma, J. K. (2007). Prediction of Fatigue Lives of Composite Material by Artificial Neural Network, Proceedings of the SEM 2007 Annual Conference and Exposition, Springfield, Massachusetts, USA, June 4–6, 2007, Copyright Society for Experimental Mechanics, Inc., Bethel, CT USA
24. National Aeronautics and Space Administration (NASA) (2010). Draft Materials, Structures, Mechanical Systems, and Manufacturing Roadmap Technology Area 12, http://www.nasa.gov/pdf/501625main_TA12-MSMSM-DRAFT-Nov2010-A.pdf
25. National Institute of Standards and Technology (NIST) (2009). Manufacturing: Accelerating the Incorporation of Materials Advances into Manufacturing Processes, Technology Innovation

Program, NIST, Gaithersburg, MD, U.S.A., http://www.nist.gov/tip/prev_competitions/upload/manuf_wp_032009.pdf
26. O' Brien-Bernini, F. (2011) Composites and Sustainability – When Green Becomes Golden, http://www.reinforcedplastics.com/view/21728/composites-and-sustainability-when-green-becomes-golden/
27. Performance Composites (2014) Material Properties for Carbon Fibers, http://www.performance-composites.com/carbonfibre/mechanicalproperties_2.asp
28. Romaniw, Y., Bras, B. (2012) Survey on Common Practices in Sustainable Aerospace Manufacturing for the Purpose of Driving Future Research, 19th CIRP International Conference on Life Cycle Engineering, Berkeley, 2012 http://www.manufacturing.gatech.edu/sites/default/files/uploads/pdf/214_Bras.pdf
29. Smith, F. (2013) The Use of Composites in Aerospace: Past, Present, and Future Challenges, http://avaloncsl.files.wordpress.com/2013/01/avalon-the-use-of-composites-in-aerospace-s.pdf
30. Sutherland, H. J., Mandell, J. F. (2004). "Updated Goodman Diagrams for Fiberglass Composite Materials Using the DOE/MSU Fatigue Database", windpower.sandia.gov/other/Global04_18983_Sutherland_Final.pdf
31. Tomblin, J. (2008) Overview of Composite Material trends in Aviation Manufacturing, Wichita State University, http://webfiles.wichita.edu/cedbr/WIRED_comp_ov_5_14_08.pdf
32. Torquato S (2000) Modeling of physical properties of composite materials. Int J Solids Struct 37:411–422
33. Verpoest, I. (2014) Composite Materials: Trends and Challenges, https://dspace.ndlr.ie/bitstream/10633/31976/1/PMC_2.pdf
34. Witten, E., John, B. (2013) Composites Market Report 2013: Market Developments, trends, Challenges and Opportunities, http://www.pultruders.com/files/pultruders.com/Documents/market_report_2013.pdf
35. Wrobel G, Kaczmarczyk J, Stabik J, Rojek M (2009) Numerical models of polymeric composite to simulate fatigue and ageing processes. J Achiev Mater Manuf Eng 34(1):31–38